

SOFIA observations of the planetary nebula NGC 7009

R. H. Rubin¹, S. W. J. Colgan¹, R. L. M. Corradi², R. Sankrit³,
A. G. G. M. Tielens⁴, Y. G. Tsamis⁵, and V. Sivaraja¹

¹NASA/Ames

²Instituto de Astrofísica de Canarias

³SOFIA Science Center

⁴Leiden Observatory

⁵ESO

Abstract. We report spectrophotometric observations made with *SOFIA*/FORCAST on 2011 June 2 UT. Optical measurements have previously shown that the abundance discrepancy factor (*adf*) varies with position in several high-*adf* PNe, and is highest close to the central star. The very low electron temperature inclusions postulated to explain the abundance discrepancy, must be cooled predominantly by fine structure IR lines. These *SOFIA* data will map mid-IR FS lines (and our related *Herschel* program will add several far-IR FS lines) in the bright, well-characterized, high-*adf* PN NGC 7009. We will compare these IR results with FS optical line measurements in order to correlate ratios of IR to optical fluxes with position, and thus correlate with where the *adf* peaks.

Keywords. ISM: abundances, planetary nebulae: individual (NGC 7009)

1. Introduction

The emission line analysis of photoionized nebulae is one of the major tools used to study elemental abundances in our own and other galaxies. Gaseous nebulae are laboratories for understanding physical processes in all emission-line sources and are probes for stellar, galactic and primordial nucleosynthesis. Because of their well defined structures and central ionizing source, PNe provide one of the best laboratories to probe the physical and astrophysical processes that affect the derivation of abundances. It is crucial to have reliable prescriptions for deriving these abundances. However, the present state of affairs continues to contain a long-standing, unsolved mystery. The ‘abundance discrepancy problem’ refers to this issue, whereby heavy element abundances relative to hydrogen derived from optical recombination lines (ORLs) are generally higher than those obtained from collisionally excited lines (CELs). Often this difference is expressed in terms of the abundance discrepancy factor (*adf*), defined as the ratio of the ORL- to the CEL-derived value. The *adf* often exceeds two in PNe (and H II regions), and is dramatically high in some PNe: ~ 5 (NGC 7009), ~ 10 (NGC 6153), 16 (NGC 2022), ~ 30 (NGC 1501), up to a factor of $\gtrsim 70$ (Hf 2-2) (Liu 2010 and references therein). Such “extreme” (*adf* $\gtrsim 5$) nebulae, albeit rare ($\sim 10\%$ of PNe surveyed), are nevertheless very important for understanding the underlying physics of the abundance determination problem.

Perhaps the most promising proposition to explain the nebular abundance problem posits that these particular nebulae contain (at least) two distinct emission regions – one of “normal” electron temperature (T_e) ~ 10000 K, and chemical composition (\sim solar) and another of very low T_e that is H-deficient, thus having high metal abundances relative to

hydrogen. The latter component emits strong heavy element ORLs and forbidden lines from the lowest-lying energy levels that give rise to IR CELs, but essentially *no optical/UV CELs*. The consistent picture that emerges from fitting a 2-abundance photoionization model to the spectroscopic data is that the H-poor component is in high-density inclusions, which provide only a minor fraction of the total nebular mass. Yuan *et al.* (2011) used the code MOCASSIN (Ercolano *et al.* 2005) to construct a detailed Monte Carlo, 3-dimensional photoionization model of the PN NGC 6153, comparing the model with a broad array of observational data, including *HST* data. The modeling including the putative low temperature, H-deficient knots does a superior job fitting the data than do models without the clumps. For any of the class of extreme PNe, it has not been possible to spatially resolve one of these knots with ground-based telescopes using state-of-the-art equipment. Tsamis *et al.* (2008) used the VLT 8.2-m/FLAMES instrument to perform integral-field spectroscopy of NGC 6153 ($0.52'' \times 0.52''$ pixels). The data are consistent with the existence of plasma regions which are *both cold and* metal-rich, appearing as undulations in the ORL abundance diagnostics of $\sim 1''$ across; any associated structures should have physical sizes of up to ~ 1000 AU.

2. How *SOFIA* observations can help

With the present *SOFIA* observations (and a similar *Herschel* program), we embark upon an alternative observational technique to test the hypothesis of the existence of such inclusions. The picture of two distinct components of highly ionized gas at very different T_e could solve the paradox, but the only known way to maintain a strongly photoionized gas at the low T_e ($\lesssim 1000$ K) expected for the clumps is by fine-structure (FS) IR line cooling. An essential check can be provided by the 2-D spatial distribution of IR FS line emission (Tsamis *et al.* 2008). Not only does *adf* vary between objects, but also for several PNe with high *adf*'s, and sufficient angular sizes, the *adf* is found to correlate with projected distance from the central star, **peaking in the inner regions**: NGC 6153 (Liu *et al.* 2000), NGC 6720 (Ring nebula) (Garnett & Dinerstein 2001) and NGC 2392 (Eskimo nebula) (see discussion p.972 in Tsamis *et al.* 2004 of Barker 1991 carbon line measurements). The basic idea is that mapping should reveal that the IR FS lines peak at the locations where the *adf* peaks in the inner regions. This sort of correlative analysis would show that large IR FS gas cooling correlates with high-*adf* positions. Optical FS lines are negligible at the low T_e of the inclusions.

3. *SOFIA* observations of NGC 7009

On a Basic Science flight 2011 June 2 UT, NGC 7009 was observed on the longest flight leg of the night (156 minutes planned). The preliminary flight plan is shown in Figure 1 with the anticipated ground track; that for NGC 7009 is leg number (16). The entire leg was flown at 43,000 feet (13,100 m), an advantage due to the lighter load which results from fuel already used. The calibration leg (17) on β And was also at 43,000 feet. Observations were made using 6 FORCAST filters: long wavelength channel (LWC) 31.5, 33.6, 34.8, 37.1; short wavelength channel (SWC) 19.7, 24.2. The transmission in these filters along with the positions of the fine structure (FS) emission lines of interest here are shown in Figure 2. These included 3 emission lines – [O IV] 25.9, [S III] 33.5, and [Ne III] 36.0 μm – as well as the underlying continuum. We knew from previous observations that [Ne V] 24.3 and [Si II] 34.8, are absent. See the *ISO* spectrum in Figure 3. The [S III] 18.7 line is expected to contribute much less than the continuum in the 19.7 filter. FORCAST covers a field of view of $3.2' \times 3.2'$ with $0.75''$ pixels, although the theoretical spatial

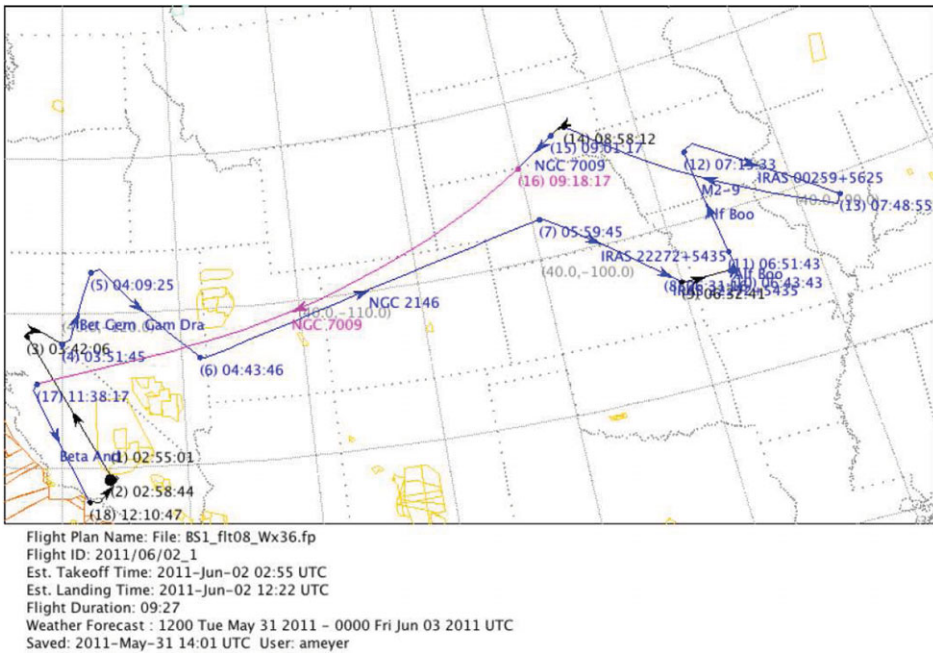


Figure 1. Preliminary flight plan. NGC 7009 was observed for the longest leg and at an altitude of 43,000 feet (13,100 m).

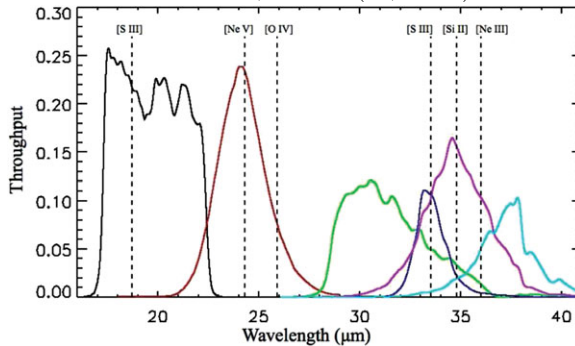


Figure 2. FORCAST filters observed: long wavelength channel (LWC) 31.5, 33.6, 34.8, 37.1; short wavelength channel (SWC) 19.7, 24.2. The positions of the fine structure (FS) emission lines discussed are indicated.

resolution near $35 \mu\text{m}$ is $\sim 3''$. As of now, the calibrated pipeline data have not yet been delivered. The resulting 2-D maps in these 3 FS lines of different ions should produce an interesting stratification with the highest ionization species O^{3+} concentrated closest to the central star. As a prelude, Figure 4 shows the preliminary accumulated data performed in real time onboard the *SOFIA* flight. One of the panels displays cross cuts along the major and minor axes for the various filters observed.

4. What we plan to do with the data next

After the calibrated pipeline data become available, we will tessellate each of the 6 filter maps to $5 \text{ pixel} \times 5 \text{ pixel}$ ($\sim 4 \text{ arcsec} \times 4 \text{ arcsec}$) spatial elements. For each spatial tile, we will then solve for 3 line fluxes – $[\text{O IV}] 25.9$, $[\text{S III}] 33.5$, and $[\text{Ne III}] 36.0 \mu\text{m}$ – as

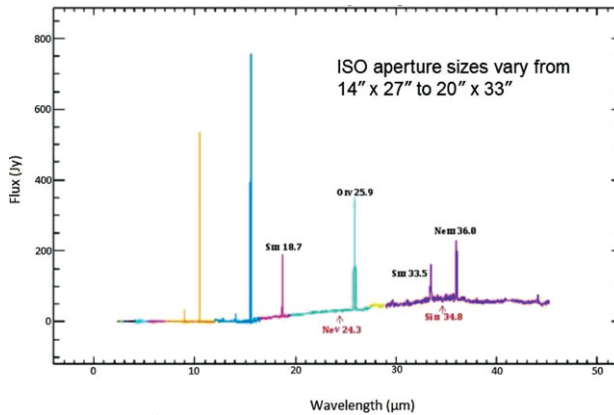


Figure 3. *ISO* spectrum SWAA73801242 that was taken in high-resolution SWS01 mode.

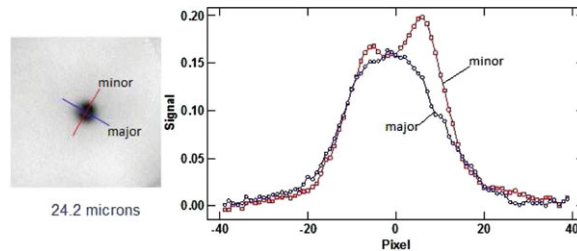


Figure 4. Onboard display of accumulated data for the SWC 24.2 filter that covers the [O IV] 25.9 μm line. These cross cuts are along the major and minor axis of NGC 7009.

well as fitting the underlying continuum with a quadratic curve. The 6 filter maps provide the values for 6 linear equations in the 6 quantities to be determined.

Armed with the maps in the three FS IR lines, as well as longer wavelength data from our *Herschel* program, we will compare these line fluxes with optical/UV CEL fluxes measured at corresponding spatial positions. For instance, there are *HST* STIS spectra and WFPC2 narrow-band images taken under GO 8114 (PI Rubin). A correlative analysis will be done to test if the flux ratio of IR to optical/UV follows the trend of variations in the *adf*.

We thank our students Vishal Kalyanasundaram, Zeyu Liu, Zezhou Liu, and Scott Zhuge for their considerable help with this project. RR is grateful for funding from the *SOFIA* Science Center.

References

- Barker, T. 1991, *ApJ*, 371, 217
 Ercolano, B., Barlow, M. J., & Storey, P. J. 2005, *MNRAS*, 362, 1038
 Garnett, D. R., & Dinerstein, H. L. 2001, *ApJ*, 558, 145
 Kingsburgh, R. L., & Barlow, M. J. 1994, *MNRAS*, 271, 257
 Liu, X.-W. 2010 (astro-ph/1001.3715)
 Liu, X.-W., *et al.* 2000, *MNRAS*, 312, 585
 Tsamis, Y. G., Barlow, M. J., Liu, X.-W., Storey, P. J., & Danziger, I. J. 2004, *MNRAS*, 353, 953
 Tsamis, Y. G., *et al.* 2008, *MNRAS*, 386, 22
 Yuan, H.-B., *et al.* 2011, *MNRAS*, 411, 1035